AD-A128 603 SCHLIEREN STUDY OF AN ELECTRIC DISCHARGE IN AN AIR FLOW 1/1
(U) NAVAL POSTGRADUATE SCHOOL MONTEREY CA T R MYERS
MAR 83

UNCLASSIFIED F/G 20/3 NL

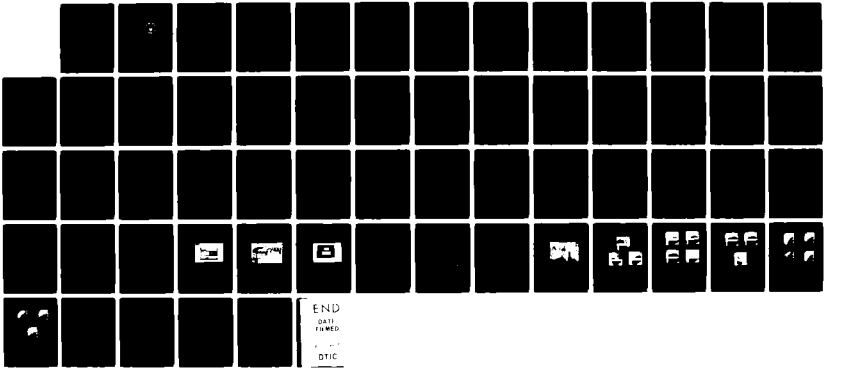

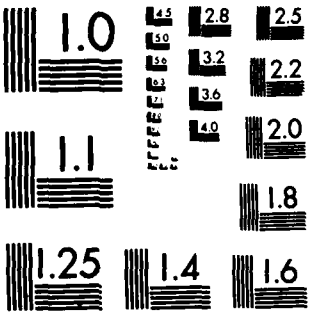

NAVAL POSTGRADUATE SCHOOL
Monterey, California

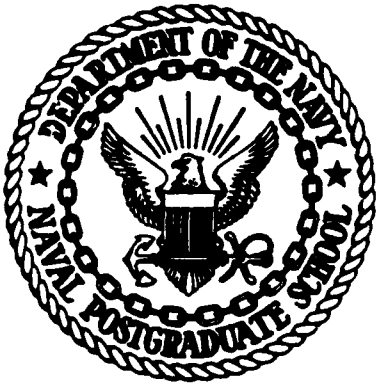

THESIS

SCHLIEREN STUDY OF AN ELECTRIC DISCHARGE IN AN AIR FLOW

by

Terry Ray Myers

March 1983

Thesis Advisor: Oscar Biblarz

SECURITY CLASSIFICATION OF THIS PAGE (When Data Entered)

REPORT DOCUMENTATION PAGE	READ INSTRUCTIONS BEFORE COMPLETING FORM
1. REPORT NUMBER	2. GOVT ACCESSION NO. AD-A128603	3. RECIPIENT'S CATALOG NUMBER
4. TITLE (and Subtitle) Schlieren Study of an Electric Discharge in an Air Flow	5. TYPE OF REPORT & PERIOD COVERED Master's Thesis March 1983
	6. PERFORMING ORG. REPORT NUMBER
7. AUTHOR(s) Terry Ray Myers	8. CONTRACT OR GRANT NUMBER(s)
9. PERFORMING ORGANIZATION NAME AND ADDRESS Naval Postgraduate School Monterey, California 93940	10. PROGRAM ELEMENT, PROJECT, TASK AREA & WORK UNIT NUMBERS
11. CONTROLLING OFFICE NAME AND ADDRESS Naval Postgraduate School Monterey, California 93940	12. REPORT DATE March 1983
	13. NUMBER OF PAGES 58
14. MONITORING AGENCY NAME & ADDRESS(if different from Controlling Office)	15. SECURITY CLASS. (of this report)
	15a. DECLASSIFICATION/DOWNGRADING SCHEDULE

16. DISTRIBUTION STATEMENT (of this Report)

Approved for public release, distribution unlimited

17. DISTRIBUTION STATEMENT (of the abstract entered in Block 20, if different from Report)

18. SUPPLEMENTARY NOTES

19. KEY WORDS (Continue on reverse side if necessary and identify by block number)

electric discharge stabilization, electrical lasers, schlieren measurement, turbulence enhancement, turbulent flow, parallel-flow electric field, cross-flow electric field

20. ABSTRACT (Continue on reverse side if necessary and identify by block number)

Performance characteristics of an electric discharge in air are examined utilizing a Schlieren system. Tests are run under flow and no flow conditions and for cross-flow/parallel-flow test sections in configurations analogous to those used in electric discharge convection lasers (EDCL's).

DD FORM 1 JAN 73 1473 EDITION OF 1 NOV 65 IS OBSOLETE
S/N 0102-014-6601

SECURITY CLASSIFICATION OF THIS PAGE (When Data Entered)

(continuation of abstract)

Results indicate that the Schlieren system is satisfactory only for flow velocities under 35 ft/sec and for currents of about 1.2 mA. Photographs of selected test runs are presented and discussed. Recommendations are made concerning more promising methods and techniques for expanding the range of conditions under which satisfactory results may be obtainable. A new design for a cross-flow test section is suggested as a result of this study.

Approved for public release; distribution unlimited

Schlieren Study of an Electric Discharge in an Air Flow

by

Terry Ray Myers
Lieutenant Commander, United States Navy
B.A., University of Florida, 1970
M.A., U.S. International University, 1978

Submitted in partial fulfillment of the requirements for the degree of

MASTER OF SCIENCE IN AERONAUTICAL ENGINEERING

from the

NAVAL POSTGRADUATE SCHOOL
March 1983

Author: Terry R. Myers

Approved by: Oscar Biblarz
Thesis Advisor

Donald P. Scuton
Chairman, Department of Aeronautics

J. D. Dyer
Dean of Science and Engineering

ABSTRACT

Performance characteristics of an electric discharge in air are examined utilizing a Schlieren system. Tests are run under flow and no flow conditions and for cross-flow/parallel-flow test sections in configurations analogous to those used in electric discharge convection lasers (EDCL's).

Results indicate that the Schlieren system is satisfactory only for flow velocities under 35 ft/sec and for currents of about 1.2 mA. Photographs of selected test runs are presented and discussed. Recommendations are made concerning more promising methods and techniques for expanding the range of conditions under which satisfactory results may be obtainable. A new design for a cross-flow test section is suggested as a result of this study.

TABLE OF CONTENTS

LIST OF TABLES

LIST OF FIGURES

ACKNOWLEDGEMENT

Although one name appears on the cover, this study is the result of the time, expertise, patience and understanding of many people. It is characteristic of these fine individuals that they perform as a team and expect only a "Thanks" from those of us whom they aid so skillfully. The author wishes to particularly thank the following: Associate Professor Oscar Biblarz for his support and direction; the technical staff of the Department of Aeronautics under the capable direction of Mssrs. Bob Besel and Ted Dunton; Avigdor Zajdman for his kind assistance in fine-tuning the Schlieren.

Finally, the love, support and understanding of my wife, Diana, and my daughters, Danielle and Heather, were most important through it all.

I. INTRODUCTION

This study is part of a continuing investigation at the Naval Postgraduate School into the properties of an electric discharge with possible applications for electric discharge convection laser devices (EDCL's). Careful scrutiny of the discharge itself may yield valuable insights for optimizing both system power and efficiency. Toward this end, a Schlieren system has been assembled to examine the behavior of an electric discharge under varying conditions and in a configuration similar to that of an EDCL.

Methods of obtaining maximum system power and efficiency are of particular interest. Since electric discharge convection lasers (EDCL's) are limited in power output by the amount of electrical power which can be coupled into the beam, so is laser gain, because it is directly proportional to the population inversion created by electrical pumping. Brown and Davis [Ref. 1] reported an optical power of 27.2 kV at a pressure of 30 Torr and at an efficiency of 17.2%. The device used was a large volume CO_2 EDCL operating in a closed-cycle mode and using combined dc and rf excitation and aerodynamic stabilization of the discharge.

There are numerous methods by which one can construct and operate electric discharge lasers. They can be differentiated by the manner in which heat is removed and the

discharge stabilized. The original set up used on CO_2 electric discharge lasers is a stagnant or no flow device which utilizes diffusion to the cavity walls as the method of heat removal. However, this method has an upper limit of 50 to 100 Watts of laser power per meter of tube length [Ref. 2]. Another type uses gas flow strictly for convective cooling [Ref. 3]. A similar one uses convective cooling with pre-ionization to accomplish discharge stabilization [Ref. 4]. A fourth type uses turbulent flow for cooling and stabilization [Ref. 5]. Eckbreth and Owen [Ref. 6] used an adjustable baffle arrangement to condition the flow by precisely controlling the flow field, velocity profile and turbulence level. This had a marked effect in delaying the onset of power-limiting instabilities. The present study seeks to examine a diagnostic tool relevant to all of the above, except those involving pre-ionization.

The use of gas flow to control heat removal and to stabilize a discharge will result in changes of temperature and density of the gas in the discharge. Numerous flow visualization techniques are available for studying the behavior of a transparent medium. The Schlieren technique has been selected in the present study because of simplicity, cost, and availability of materials. Cross-flow and parallel-flow configurations have been examined under flow and no-flow conditions. The electrode configurations for cross-flow and parallel-flow are shown in Figures 1 and 2, respectively.

Shwartz and Wasserstrom [Ref. 7] note that the power capability of an electric discharge convection laser (EDCL) is scalable with mass flow rate. Mass flow rate can be increased by increasing density (ρ), velocity (V) or discharge area (A), although elevated pressures associated with increasing density do cause difficulty with the discharge stability. They also state that the temperature of the lasing medium is one of the most critical parameters affecting molecular laser performance and that turbulence produces a more uniform gas temperature distribution which in turn produces a more stable discharge. They credit Shwartz and Margalith [Ref. 8] with showing that $\dot{m}/L$ (mass flow rate divided by the discharge length as measured in the flow direction) determines the relative importance of conduction and convection in transporting waste energy out of the laser cavity. Finally, they state that reduction in gas temperature, at a given power loading, results in a corresponding increase in the vibrational temperature and population of the upper laser energy level [Ref. 9].

Post [Ref. 10] studied the effect of sub-ambient controlled turbulent air flow on discharge performance utilizing thin rectangular plates with holes in them to generate the turbulence. Experimental results yielded plates with 50% area blockage (Fig. 3) that generated the most turbulence. Post concluded that as mass flow rate increased, convective cooling, turbulence, and density increased resulting in a more stable discharge and thus in

greater discharge power. He reported more than twice the energy per unit mass was obtained for sub-ambient turbulent flow at approximately half the mass flow rate of atmospheric non-turbulent flow. Post [Ref. 11] also reported an intense, short, narrow glow extending from the anode tips which was described as a region of high current density. Activation of the turbulent flow caused this region at the tips to widen and become visibly more dispersed so that the localized current density in that region becomes more diffused due to the effects of turbulent mixing. The combined effect of reduced pressure and turbulent flow was observed to increase discharge power by 750% over ambient laminar flow at the same mass flow rate.

Barto [Ref. 12], in a companion study to Post's work, studied the effects of variation of discharge parameters on the voltage-current characteristics of the multi-pin electrode arrangements used. These included gap width, flow speed, turbulence intensity, electrode orientation, rate of voltage increase, and gas density. Barto [Ref. 13] developed a model of the flow-discharge interaction mechanism. The flow field interacts with the charged particles produced in the discharge region and changes the shape and extent of the space charge region by convection and turbulence. Many variables impinge on the gross behavior of the system voltage and current, such as gas transit times, turbulent fluctuation times of density and velocity,

ionization and recombination times, and streamer propagation and growth times.

The three charged particles of primary interest are positive and negative ions and free electrons. Due to their small mass, electrons have relatively high mobility and gas convection does not interact significantly with the electrons. Ions, however, are much more massive and ion drift velocities can be of the same order of magnitude as the flow velocity. High densities of charged particles produce electrostatic fields of their own which can reach the same order of magnitude as the applied field, which implies that electrons are indirectly affected by convection through the alteration of the electric field structure by the movement of high density ionic space charges. Visual observation of a discharge easily shows the ability of turbulent flow to affect the luminous regions of the discharge.

Turbulence is a phenomenon characterized by fluctuating, time-dependent variations in gas density. The turbulent spectrum may vary from 100 Hz to 20 kHZ in the discharge region. The characteristic times associated with the turbulence are on the order of 1×10^{-2} to 5×10^{-5}sec ($\tau = 1/f$, where f is the frequency of the turbulence). These times are long compared to the characteristic times associated with charged particle kinetic processes, with the result that charged particle properties adjust in a quasi-steady fashion to fluctuations in gas properties.

Charged particle kinetics and energy transfer processes couple to fluctuations in the neutral gas primarily through changes in gas temperature and density. This suggests the efficacy of utilizing a Schlieren system to investigate these phenomena. Turbulent fluctuations in temperature or density can cause substantial increases in current due to the quasi-steady coupling of electron kinetics to temporal variations of neutral gas properties. Local increases in electron current density can have a large destabilizing effect on the discharge since increased current density causes increased joule heating of the gas. Turbulence enhances ionization by significantly increasing the average effective ionization coefficient, which has an exponential dependence on reduced pressure and density [Ref. 14]. Since the strongest density fluctuations are accompanied by the highest fluctuating velocity components, which tend to disperse concentrations of space charge and dissipate local hot spots, it also acts to prevent unstable runaway conditions from developing due to the formation of local hot spots in the gas. It homogenizes the discharge region and creates a much larger ionization region at the anode, which is a major source of additional current.

The basic geometric design of the electrodes used in this study is that of the familiar positive point-to-plane, which is often used in electric discharge work (see Figures 1 and 2). The point-to-plane discharge can be divided into

distinct regions due to the divergence of the applied electric field distribution. The first is an intense region of ionization near the point. The second is a space charge region fed from the ionization region by electrostatic repulsion of positive ions. The third is the quasi-neutral region in which the applied electric field has dropped below the value required for appreciable ionization activity. This region is disturbed more and more by the intrusion of pre-breakdown streamers as gap breakdown is approached. The maximum length of these streamers is proportional to the applied voltage.

Barto's space charge model [Ref. 15] is based on the dynamic processes which occur when the gap is very near breakdown potential. Under these conditions, a positive point-to-plane gap in an electronegative gas experiences a pulsating current due to formation of pre-breakdown streamers which vary in a statistical manner.

In a uniform electric field between parallel plates, the field strength is inversely proportional to the plate spacing:

$$E = V/d \tag{1}$$

where V is the applied voltage and d is the electrode spacing. If the anode could be made to emit positive ions, and if the bulk of the discharge is electrically neutral, there will be a small region near the anode in which the ion density exceeds the neutral charge density. A net

positive charge will characterize this area and the effect of this is to lower the electric field in this area. If intense space charge exists, a "virtual anode" is created [Ref. 16] where the voltage increases (voltage gradient is initially positive). If this is so, the apparent physical gap length is reduced by space charge modification of the electric field structure. Barto [Ref. 17] gives an approximate relation for the breakdown field strength as:

$$E = (V/d) * (1 + (\delta/d)) \qquad (2)$$

where V is the breakdown voltage, d is the electrode spacing and δ is the distance of the virtual anode from the origin. The basic physical mechanism of current production in a gaseous discharge is the electron avalanche. Very small changes in the electric field structure by space charge convection can cause large changes in current.

Barto [Ref. 18] concluded that his space charge model was reasonable and that gasdynamic interaction promoted stability of a discharge in several ways: pure convection, density reduction, and turbulence. The basic mechanism of all of these appears to be through thermal stabilization by heat removal from potentially developing hot spots in the gas. He also reports that high intensity, low frequency turbulence was best for stabilization and, in conjunction with Post, that a system with a diffuser and turbulence generating screen developed a much higher power input at a lower mass flow rate than those not so equipped. His major

recommendation is that current distribution studies should be performed for correlation with temperature profiles as well as breakdown location statistics and turbulence and velocity profile measurements. The present study, as a result, attempts to examine the temperature profiles of the discharge under various conditions and configurations.

In a more recent study, Barto [Ref. 19] examined gas dynamic stabilization of high pressure, highly non-uniform electrical discharges using two different electrode geometries. The geometries studied were the multiple-point to plane (of the type used in the present study) and the multiple-wire to plane. Preliminary analysis indicated the potential for improving the discharge input power by a factor of 2-3 times with the wire anode. However, due to power supply limitations, no improvement in performance was noted. Nonetheless, it was found that the transition from the high field to the drift field is well defined for a sharp point, but becomes very slow and indefinite in wires. This results in a change in the behavior of breakdown voltage as a function of velocity such that the curves for the breakdown voltage show an upturn toward the asymptote at a low velocity whether or not the flow is turbulent. The wire geometry also has inherently higher values of electric field in the drift region of the gap and an increased ionization volume which spans the length of the wires. It was concluded that the anode extension model

appears to offer a simple and effective approach to the interpretation and calculation of basic gas dynamic effects on high pressure corona discharges and that this modelling approach can be applied to other gap configurations, polarities, gas mixtures and pressure regimes.

Aunchman [Ref. 20] reiterates that EDCL's use relatively safe gases (CO_2, N_2, He) and offer good potential in efficiency and power levels. He also mentions that charge build-up at the electrode is the cause of arcing or breakdown of the discharge. Turbulence mixes and spreads out the charge concentration that builds up at the electrode. He proposes a closed-cycle system design that continuously recirculates and reuses the laser gases with the advantages that one can control the velocities, temperatures, pressures, etc., of the constituent gases and that one does not waste precious gases such as helium. Two notable effects of turbulence take place in the discharge, mixing due to turbulence (the more important effect) and convection. He found that the intensity of turbulence in the discharge region seemed to be a function of flow blockage, with 50% blockage appearing to be optimum.

Biblarz, Barto and Post [Ref. 21] build on importance of gas dynamic stabilization as a means of increasing power into diffuse discharges in molecular gases such as are found in molecular lasers, MHD devices, atmospheric discharges, etc. Turbulence, vorticity, and supersonic

flow with shocks have been observed to cause bulk convective cooling and the interaction between the flow field and ions which affects the fundamental nature of the glow discharge. Corona inception voltage and breakdown voltage are modified by the flow. Simultaneously, current becomes considerably more homogeneous and greatly enhanced. Reference 21 reports on factors influencing the discharge such as, convective velocity, density, interelectrode spacing and electrode orientation. They noted that convective velocity had a stabilizing effect on the discharge and that there was an increase in current and velocity nearly proportional to the square of the convective velocity. They also state that gas dynamic phenoma have characteristic times comparable to recombination time, current pulsing, and ion drift times. Since ion drift time is not much faster than flow times, one can surmise that within the virtual anode or anode extension region, convection is significant. Their experimental results indicate that factors which affect breakdown voltage most significantly are density, velocity, and turbulence. The factors which most strongly affect breakdown or maximum diffuse current are turbulence and velocity. The behavior of maximum power follows closely that of current, the change in magnitude of the voltage being relatively small. Power into the discharge is enhanced by 500 times through the combined action of flow, turbulence, and reduced density.

Davis [Ref. 22] also studied aerodynamic stabilization of an electric discharge in air for potential use with gas lasers, with particular emphasis on the CO_2 laser. Energy is stored in the CO_2 molecule in three electronic states, rotation, vibration, and translation. These forms of energy can be assigned a specific value representing a particular energy level. The number of molecules excited to a particular energy level can be predicted at equilibrium using Boltzman statistics. An important criterion for lasing is the achievement of a population inversion which occurs when the number of molecules excited to a higher energy level exceeds the number of molecules at a lower level. Maximum laser power is proportional to the population inversion. This is controlled by the amount of electric power that excites molecules to states that eventually lase. Davis [Ref. 23] used pulsating jets to generate the low frequency turbulence spectrum to stabilize the discharge.

Wainionpaa [Ref. 24] also studied the problem of electric discharge performance in both parallel and cross-flow electric fields. He reiterates that while maximum diffuse power is desired, the major limitation on this is the arc discharge through the medium. The gaseous medium itself, the material and geometry of the electrodes and the conditions of flow all influence the onset of arcing. The effects of arcing are numerous. Resistance and dielectric

strength diminish markedly, high current flows, the electric field collapses and damage to the electrodes may occur. Wainionpaa [Ref. 25] found that the source of turbulence should be placed as near as possible to the discharge region to optimize turbulence stabilization of the discharge. He also found that an even, round, pinkish-orange glow was evident at the tipmost third of the conical end of each pin of the anodes in both flow and no-flow conditions. Additionally, in both parallel and cross-flow configurations, the no-flow conditions were symmetric about the center row of pins and identical in appearance with regard to intensity, color, width, diffuseness and the shape of the glows for the same interelectrode gap dimension. He observed the mechanism of breakdown as being a multitude of arcs which spanned the interelectrode gap and which appeared to originate randomly from different pins in the pin-rack anodes in all flow conditions. Increased stabilization of the discharge by flow of the medium was obtained in all cases. The faster the flow, the greater the power into the discharge with the increase being normally greater than linear. Turbulence further stabilized the discharge, unless the gap between anode and cathode became too large. The parallel-flow configuration had higher power capacity than cross-flow. A schematic diagram of the cross-flow configuration appears in Figure 4. The upstream row of pins had the greatest amount of turbulence acting on it with the downstream rows having progressively less.

Because of this, the upstream row experienced a marked growth in glow compared to the downstream rows. When the corona first becomes visible, glow extends from row 1 almost anti-parallel to the flow, tilted slightly toward the cathode. As the voltage increases, the glow from row 1 bends downward and a glow begins at row 3. Further increases in voltage cause the glow from row 3 to become nearly as bright as row 1 and the side view of the discharge is symmetric with respect to row 2 with only a faint glow from the center row. All pins have a round pinkish-orange glow at this point. Higher voltage causes the glow from row 1 to become more dominant, the glow of row 2 increases in width and brightness, while row 3 diminishes in intensity. Just prior to breakdown almost no glow is visible from row 3, except that at the very tip of the pins. At this point, streamers or sparks become visible in the row 1 glow, but they are not strong enough to cause the arc breakdown. Increasing voltage more causes breakdown to occur.

Nainionpaa [Ref. 26] concluded that maximum power was obtainable from the parallel-flow configuration with a maximum interelectrode gap of 4.8 cm at a turbulent flow of 60 m/sec. Flow enhanced discharge stabilization in all experiments.

Tucker [Ref. 27] explored the possibility of enhancing the electrical power handling capabilities of a flowing gas

by means of acoustically generated disturbances. Equipment failure precluded gathering meaningful data in this area. However, he noted that previous works indicated the feasibility of the method and that benefits from resulting disturbances in the flow would improve the system performance. Tucker also conducted follow-on research which verified the results of Wainionpaa [Ref. 28]. Tucker [Ref. 29] used an oscilloscope to measure the current through the downstream cathode with respect to time. Results showed a series of spikes whose time density appeared to be solely a function of flow rate of the gas as opposed to electrode spacing or power applied to the electrodes. He thought that this might imply a flow-related current pulsation which may ultimately be related to turbulence.

B. THE SCHLIEREN METHOD

The Schlieren method provides a unique and important tool for the investigation of flow of gases with particular application to the study of heat transfer, shock waves and other phenomena. It is commonly used to study flow patterns about aerodynamic surfaces. It was first discovered over one hundred years ago by Foucault and Toepler. The word "Schlieren" comes from German and means "streaks or striations" [Ref. 30]. It is one of several optical methods which consist of a parallel or divergent light beam which passes through a set of lenses, mirrors, viewing windows

and the flow field. The interactions of the flow and the test object cause a change in the thermodynamic state of the gas, notably the density. The change of density produces a change in the refractive index of the medium which results in an optical disturbance that manifests itself in the schlieren pattern. The simultaneously occurring alterations with respect to the undisturbed case are of two types: (1) the ray is deflected from its original direction or (2) the phase of the disturbed ray is shifted from respect to that of the undisturbed rays. Merzkirch [Ref. 31] states that the optical behavior of an ionizing gas is dominated by the presence of free electrons, even at a low ionization level. The Schlieren method measures the angular deflection of the disturbed ray with respect to the undisturbed ray. It is sensitive to changes of the density gradient. Weak changes in density result in changes due to refractive deflection and changes due to diffraction being of the same order of magnitude. Diffraction, therefore, determines the sensitivity limits of flow visualization methods making use of light deflection.

There are many methods for arranging and utilizing a Schlieren system. The one used in this study is shown schematically in Figure 5.

II. EXPERIMENTAL APPARATUS

The experimental apparatus is divided into three subsystems, namely, the flow system, the discharge system, and the Schlieren system.

A. FLOW SYSTEM

The flow system is composed of an air compressor, water-cooled heat exchanger, flow rate control valves, a plenum chamber, a converging nozzle to the test section, and turbulence generating plates. A schematic diagram of this system appears in Figure 6. The turbulence plates, however, were not used in this work for reasons addressed in a later section.

A three stage Carrier centrifugal compressor provides air flow at a maximum rate of 4000 cubic feet per minute and at a maximum pressure of two atmospheres. The air is passed through a water-cooled heat exchanger which maintains flow temperature at 90° F. Flow is regulated by three gate valves and is exhausted directly into the atmosphere from the test sections.

Air flow is measured using a pitot-static probe mounted to the flow exit area and outside the boundary layer. An inclined, colored water manometer is used to display pressures.

The cross-sectional constant areas of the test sections are both 2.22 x 4.44 inches. The electrode orientation is

altered by 90 degrees in the cross-flow section which is somewhat longer in order to hold an additional cathode plate downstream. Wainionpaa [Ref. 32] found that the downstream cathode was detrimental to cross-flow power capacity. Therefore, the additional cathode plate was not used in this study.

B. DISCHARGE SYSTEM

The discharge system consists of a high-voltage power supply with associate high power leads, the pin anodes, the rectangular plane cathodes, and current and voltage measuring devices.

The power supply is a Universal Voltronics Labtrol Model BA 50-70 capable of providing up to 50 kilovolts at 70 milliamperes direct current. It consists of a control unit and a high voltage output cannister. The control unit is internally protected and breaks the current when either the output voltage exceeds 50 kilovolts or the current exceeds 70 milliamperes. These values may be individually adjusted to lower levels to suit the needs of the operator. A voltmeter and an ammeter are contained within the control unit.

The output of the high-voltage cannister is connected to a polished brass sphere by a high voltage cable supplied by the factory. The sphere is immersed in a high dielectric oil bath to prevent arcing. All equipment is well-grounded to a common laboratory ground.

The anode consists of three rows of thirteen unballasted stainless steel pins connected in common. In the parallel-flow configuration the cathode is brass and consists of a grid which effectively presents a plane of ground potential to the anode while providing minimum blockage of the flow. In the cross-flow configuration the cathode is a 2.22 x 4.44 inch stainless steel plate one-sixteenth of an inch thick.

C. SCHLIEREN SYSTEM

The Schlieren system consists of two optical benches, a mercury vapor light source with adjustable focal length, two knife-edges, two sets of thin-lens combinations, two plane front surface mirrors, a remote-controlled shutter, and a camera body with film holder. The optical benches provide mounting supports for the equipment, the plane mirrors control the direction of the light beam and the thin-lens combinations collimate and focus the beam where desired. The first knife-edge serves to define a sharp boundary in the light beam and the second one is used to adjust the sensitivity of the system. There are numerous methods for arrangement of Schlieren components and a variety of the more common configurations may be found in Babits [Ref. 33], Reid [Ref. 34], Vasil'ev [Ref. 35], and Merzkirch [Ref. 36]. The physical constraints of the laboratory prompted the selection of a U-shaped system in this study. The system is shown schematically in Figure 5 and photographically in Figure 7.

III. PROCEDURE

The major components of the flow and discharge systems used in this study had been designed, assembled, and used in previous studies (Post [Ref. 37], Barto [Ref. 38], Wainionpaa [Ref. 39], and Tucker [Ref. 40]). The first step in the procedure, then, was to select either the parallel-flow or cross-flow configuration and mount it on the flow system. With the desired test section installed, the continuity of the discharge circuit was checked and proper grounding of the equipment was confirmed. Upon satisfactory completion of these checks, the discharge and flow systems were essentially ready for conducting tests. Prior to conducting any runs, however, it was necessary to modify the test sections in order to be able to perform Schlieren measurements. In the case of the cross-flow configuration, Schlieren quality rectangular glass windows were cut to size and installed in place of existing plexiglass windows. These were placed in the sides of the test section to permit the beam to pass through the test section parallel to the pin anode rows undistorted and at the same time prevent any flow from escaping through the side walls of the test section (see Figure 1). In the case of the parallel flow configuration, similar plexiglass windows

were removed, but, because it was decided to conduct the runs with this test section at relatively low flow rates, no glass was reinserted. No detrimental effects were encountered due to running the system in this manner (see Figure 2). Once all of the above steps were accomplished, it remained to mount, align and adjust the Schlieren system for proper sensitivity, as well as to install the photographic equipment and to ensure its proper operation. These procedures are covered in detail below.

A. SCHLIEREN SYSTEM ALIGNMENT AND SENSITIVITY ADJUSTMENTS

For purposes of clarity in this discussion, assume that a right-handed orthogonal coordinate system is located with its origin, O, at the light source. The positive x-direction is in the direction in which the light beam is traveling, the positive z-direction is vertically up (away) from the center of the earth), and the positive y-direction is normal to each of these according to the right hand rule. Additionally, "downbeam" refers to the positive x-direction and "upbeam" refers to the negative x-direction, or towards the light source.

As previously mentioned, the system was assembled in a U-shaped manner due to laboratory space constraints (see Figures 5 and 7). This is merely a simple variation of the ubiquitous z-shaped system, with the light ray passing through the test section only once. Tables were constructed to hold the optical benches and electronic equipment in a

compact arrangement at the height of the test section. Adjustable mounts for each component of the Schlieren system were assembled and fitted locally. The adjustable mounts permitted each component to be swivelled 360 degrees in the x-y plane and moved 2 to 3 inches vertically in the x-z plane. All mounts had set screws permitting firm attachment and holding of all movable parts once proper alignment had been achieved.

The machining of the benches was of sufficient accuracy to permit alignment along the x-axis, with the swivel adjustment feature of the mounts permitting accurate alignment.

The first step in the alignment process was to adjust each component properly in the z-direction. The major constraint in this phase was the height of the test section. The first element to be set to this height was the light source. Each succeeding element was then set in order downstream of the light source. An ordinary piece of cardboard was used to follow the beam and to ensure that it traversed the test section as desired.

The next step was to determine the focal lengths of the lens of the light source as well as that of each of the combination lenses. It was desirable to use appropriate thin-lens combination formulas [Ref. 41] for this purpose, however, the thin-lens combinations had been previously assembled from lenses of unknown properties

without focal length information on assembly, and as these were the only ones available, it remained to determine the focal lengths experimentally.

This latter step having been performed, the first knife edge was placed at the focal point of the light source lens. The first thin-lens combination was then adjusted upbeam and downbeam until the image of the test section formed by the light beam passing through it and the thin-lens combination was focused at infinity. This was done so as to ensure that the rays passing through the test section were essentially parallel. A rough method to ensure that this was indeed the case was to measure the diameter of the light beam before and after it passed through the test section. It proved to be the same in both cases.

Once a parallel beam through the test section had been achieved, the second thin-lens combination was moved upbeam and downbeam until the second knife edge was exactly at the focal point of this thin-lens combination. The shutter was then left open and the camera body was placed so that the image of the test section fell on the plane in which the film was mounted.

Finally, the second knife edge was used to cut off most of the point of light that was focused on it by the second thin lens combination. It was helpful for this knife edge to be able to be finely adjusted by vernier knobs in both the z- and y-directions. It was important to ensure that

the knife edge was perpendicular to the light beam. The technique which gave the best results was to totally block the light beam with the knife edge and then slowly let in more and more of it until the test section was just visible. It was quite possible to ensure the rough sensitivity of the system by making certain that one could view the changes in density due to the heat caused by friction of the thumb and forefinger held just under the light beam on the downbeam side of the test section.

B. PHOTOGRAPHIC PROCEDURE

The film utilized for the Schlieren photographs was Polaroid ASA 55 film. Prior to each picture, a single piece of film was loaded into the camera back. A remote shutter control was placed next to the high voltage power supply and was activated when desired flow and power conditions had been achieved. A minor inconvenience was experienced due to the necessity of having to readjust the second knife edge for proper sensitivity and alignment each time the film was loaded. This is further addressed in a later section.

C. PERFORMING A TEST RUN

Once the Schlieren system had been adjusted to the proper sensitivity and the photographic apparatus set, the flow system was set to the desired speed by opening a gate valve until a desired height differential was obtained

on the fluid manometer being used. A number of pictures were taken corresponding to each different voltage level desired. The procedure was then repeated at the next desired set of flow conditions.

IV. RESULTS AND DISCUSSION

A. CROSS-FLOW CONFIGURATION

The first series of runs were conducted using the cross-flow configuration. Photographic results are displayed in Figures 8 through 10. Flow conditions for each picture are summarized in Table I. Flow is from right to left in all cases.

Figure 8a shows the test section with no flow and no applied voltage. The Schlieren pattern is caused by a candle held just downbeam of the test section and below the light beam.

A heated soldering iron was placed inside the test section as a second check on sensitivity with flow. This photograph appears as Figure 8b. A slight Schlieren pattern is visible. It was found, however, that a stronger Schlieren pattern was obtainable if one slightly disturbed the air mass inside the test section, either by fanning one's hand over the exit or blowing into it. Figure 8c presents the same heated soldering iron with a flow rate of 33.1 ft/sec applied to the test section. A Schlieren pattern is slightly discernable around the soldering iron, almost conforming to the exact shape of the soldering iron itself. It became clear at this point that a delicate balance would have to be struck between desired flow conditions and desired Schlieren

display. Some slight flow was needed to ensure sufficient current flow and an acceptable Schlieren image, however, a flow greater than about 35 ft/sec would preclude any Schlieren pattern due to the quick convective removal and dissipation of heat energy and the concurrent homogenizing effect this had on density throughout the test sections.

Higher flow rates result in higher currents which in turn causes higher amounts of joule heating of the gas. However, convective cooling is also increased. The joule heating is proportional to velocity squared while the convective cooling is proportional to the square root of the velocity for laminar flow and to about the 3/4 power of velocity for turbulent flow. At lower flow rates, the effects of velocity on convective cooling and joule heating are similar.

Flow velocity was reduced to 23.39 ft/sec and a second series of pictures were taken, this time with a voltage applied to the electrodes. Figure 9a was made with 19.5 kV applied and a resulting current of 1.2 mA. A thin cone-shaped area 3 degrees wide is barely visible extending from the tip of the row one anodes almost parallel to the flow and extending to and partially engulfing rows 2 and 3. Figures 9b and 9c were made under the same flow conditions, but immediately prior to breakdown.

Flow velocity was again reduced to half of the original velocity, or 16.34 ft/sec. Figure 9d was made at 19 kV and

1 mA. Figures 10a and 10b were made immediately prior to breakdown. All three of these latter pictures show a 5 degree cone which widens as it extends from the tip of the row 1 anodes to and past the downstream rows. Each row in turn adds its own thermal energy to this region and further influences conditions at the downstream row. One could speculate from this that since the row 3 pins were farthest downstream and obviously received additional thermal energy through flow convection from rows 1 and 2, that row 3 would be more prone to local instabilities and hot spots breakdown arcing would occur. This was not the case. Arcing appeared to occur randomly within the three rows, with no site seeming to be preferred.

It proved quite difficult to photograph breakdown arcs just as they occured. However, Figure 10c shows the test section immediately after an arc had occurred in the center row of pins. The picture was taken under no-flow conditions. Strong thermal activity in the area of arcing is indicated.

B. PARALLEL-FLOW CONFIGURATION

The next series of runs was conducted utilizing the parallel-flow configuration. These results are photographically displayed in Figures 11 and 12. Flow conditions are summarized in Table II. Flow direction is from right to left.

Figure 11a shows the test section with no flow and 25 kV applied resulting in a current of 0.25 mA. No visible pattern resulted. Figures 11b and 11c were also taken under conditions of no flow, but with applied voltages of 26.5 kV applied resulting in a current of 0.25 mA. No visible pattern resulted. Figures 11b and 11c were also taken under conditions of no flow, but with applied voltages of 26.5 kV and 27.0 kV, respectively. These voltages resulted in a current of 0.8 mA in both cases. The upper row exhibits a striking Schlieren pattern in both figures, while the other rows appear to exhibit little activity. Note that the thermal activity of one row of pins (in this case the upper) has somewhat less influence on the next row as compared with the cross-flow configuration. That is, the thermal energy from one row is not entirely diffused into the next row. This may be a partial explanation for the higher values for breakdown voltage for a given flow velocity in the parallel-flow case. Figure 11d was taken immediately prior to breakdown under no-flow conditions. The thermal activity is confined mainly to the center row of pins this time and there is a tendency for the general shape of this region to be that of a paraboloid of revolution.

In Figure 12a, a flow velocity of 16.54 ft/sec was established with an applied voltage of 26.5 kV and a resulting current of 0.8 mA. Thermal activity, even at this low velocity, is almost completely indiscernable.

In Figure 12b, the flow velocity has been increased to 23.39 ft/sec and a voltage of 28 kV with a current of 0.8 mA applied. Some type of streamer activity is visible emanating from the upper row of pins. This is the only visible activity.

Figure 12c shows a faint conical region of activity 8 degrees wide extending from the bottom row of pins. Flow velocity was 33.08 ft/sec at 28 kV and 0.8 mA.

Further testing on both the parallel and cross-flow configurations will have to wait for a Schlieren system able to discern density changes at flow velocities above the relatively low value of 35 ft/sec. The effects of heat convection by even these low flow rates was substantial enough to render the Schlieren system useless, except perhaps in the immediate boundary layer at the tip of the pins, but considerably greater resolution would be required for this. At the higher velocities at which the effects of turbulence and convection become particularly pronounced, where it was hoped the Schlieren system would provide some clues regarding the structure and behavior of the discharge under conditions of high power, high flow velocities, and strong levels of turbulence, the available Schlieren system proved inadequate.

V. CONCLUSIONS AND RECOMMENDATIONS

It has been verified that use of optical techniques is a valid method for investigation of an electrical discharge in a flowing gaseous medium. The results of this study suggest that the Schlieren method is sound and has the potential for providing additional insights into the mechanisms and processes which influence electric discharge behavior. The main problem to be overcome appears to be reconciling magnitude of power and flow desired with sensitivity of the optical system. It is recommended that an interferometer or Schlieren-interferometer system be utilized to enhance optical system sensitivity. It may prove profitable to utilize a low power laser as the light source in the above systems. (Kogelschatz and Schneider [Ref. 42] discuss a quantitative laser-Schlieren technique applied to high current arc investigation. Narrow-band interference filters permitted suppression of the intense radiation of the arc itself, including the highly luminous arc core.) It may also prove fruitful to use holographic techniques in conjunction with an interferometer system.

It is also concluded that convection of thermal energy from upstream pins to downstream pins in the cross-flow configuration may have an adverse effect upon the performance of this configuration. Redesign of the cross flow

configuration is recommended to investigate the effects of staggering the pins so that minimizing or eliminating the effects of convection of thermal energy from upstream pins may be examined. If there is a cause-effect relationship, such a design should result in increased performance for the cross-flow configuration.

Finally, some difficulty was encountered due to the mounting of the camera on the same bench as the downstream mirror, thin-lens combination, and knife-edge. Each loading and unloading of film required readjustment of the knife-edge to ensure proper sensitivity. It is recommended that future systems have a camera mounted on a separate bench or table to preclude the necessity for continuous readjustment of the system, or a better camera be acquired.

Table I. Flow Condition Summary (Cross-Flow Set-Up)

Figure #	V (kV)	I (mA)	h ("H_2O)	U (ft/sec)
8a	0	0	0	0
8b	0	0	0	0
8c	0	0	0.5	33.08
9a	19.5	1.2	0.25	23.39
9b	Breakdown		0.25	23.39
9c	Breakdown		0.25	23.39
9d	19.0	1.0	0.125	16.54
10a	Breakdown		0.125	16.54
10b	Breakdown		0.125	16.54
10c	Breakdown		0	0

Table II. Flow Condition Summary (Parallel-Flow Set-Up)

Figure #	V (kV)	I (mA)	h ("H_2O)	U (ft/sec)
11a	25.0	0.25	0	0
11b	26.5	0.8	0	0
11c	27.0	0.8	0	0
11d	Breakdown		0	0
12a	26.5	0.8	0.125	16.54
12b	28.0	0.8	0.25	23.39
12c	28.0	0.8	0.5	33.08

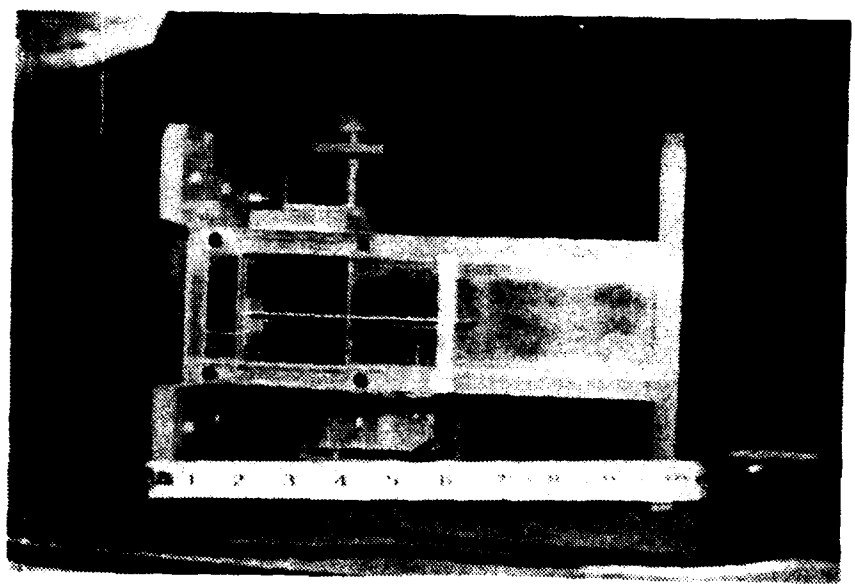

Figure 1. Cross-Flow Configuration Test Section

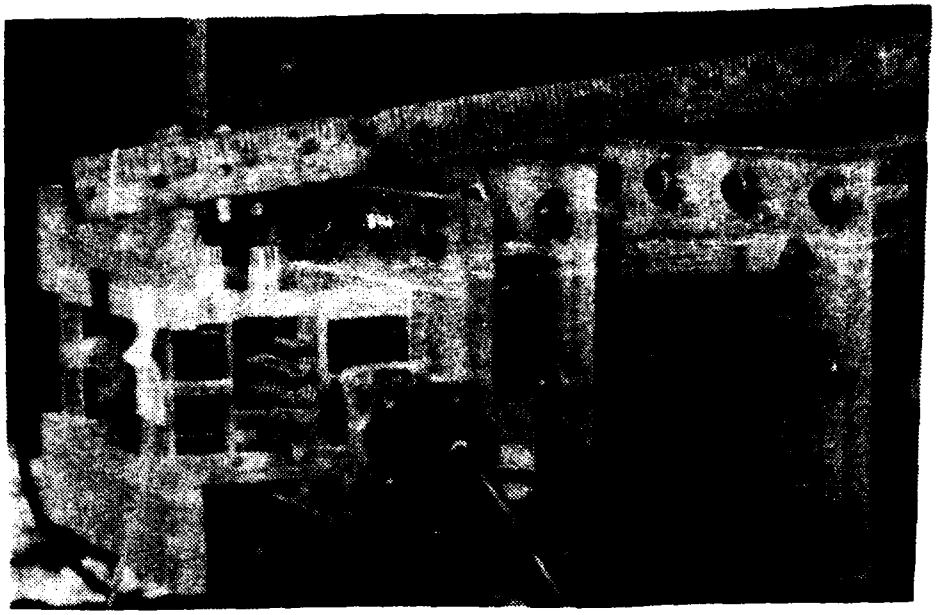

Figure 2. Parallel-Flow Configuration Test Section

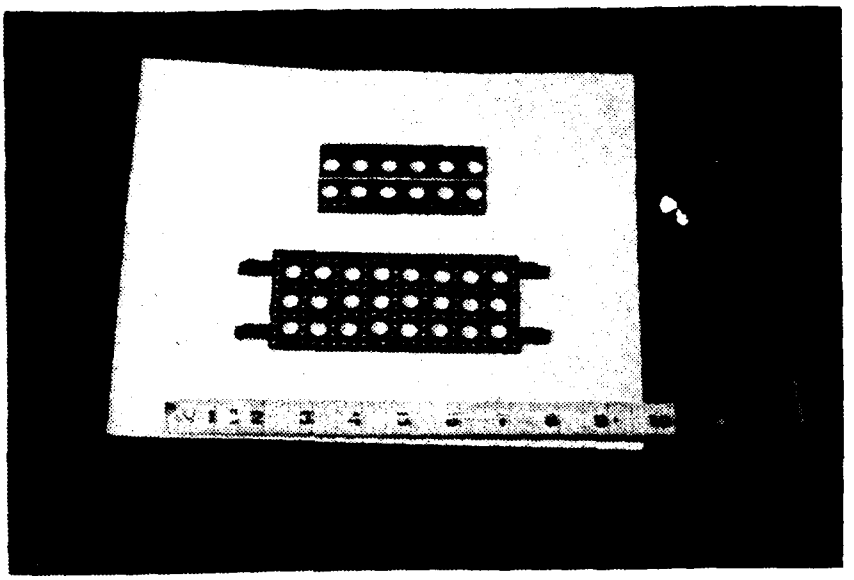

Figure 3. Turbulence Generating Plates [Ref. 10]

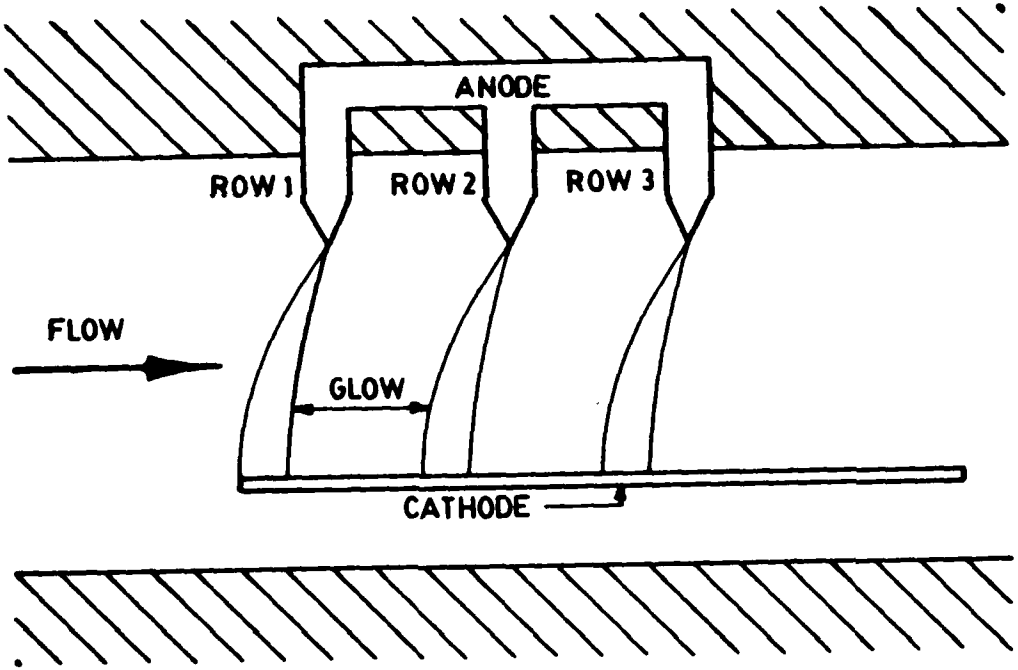

Figure 4. Cross-Flow Configuration Schematic

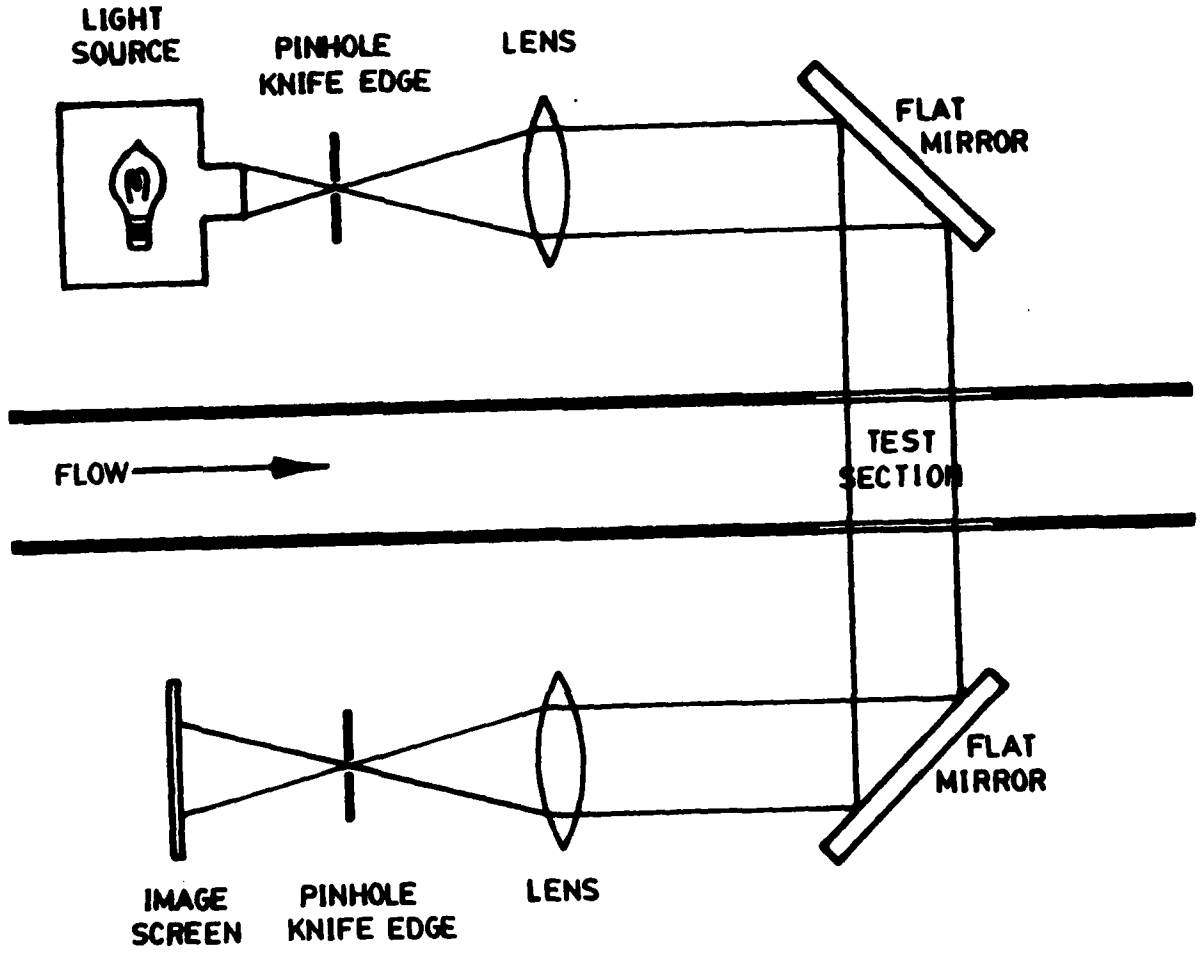

Figure 5. Schlieren System Schematic

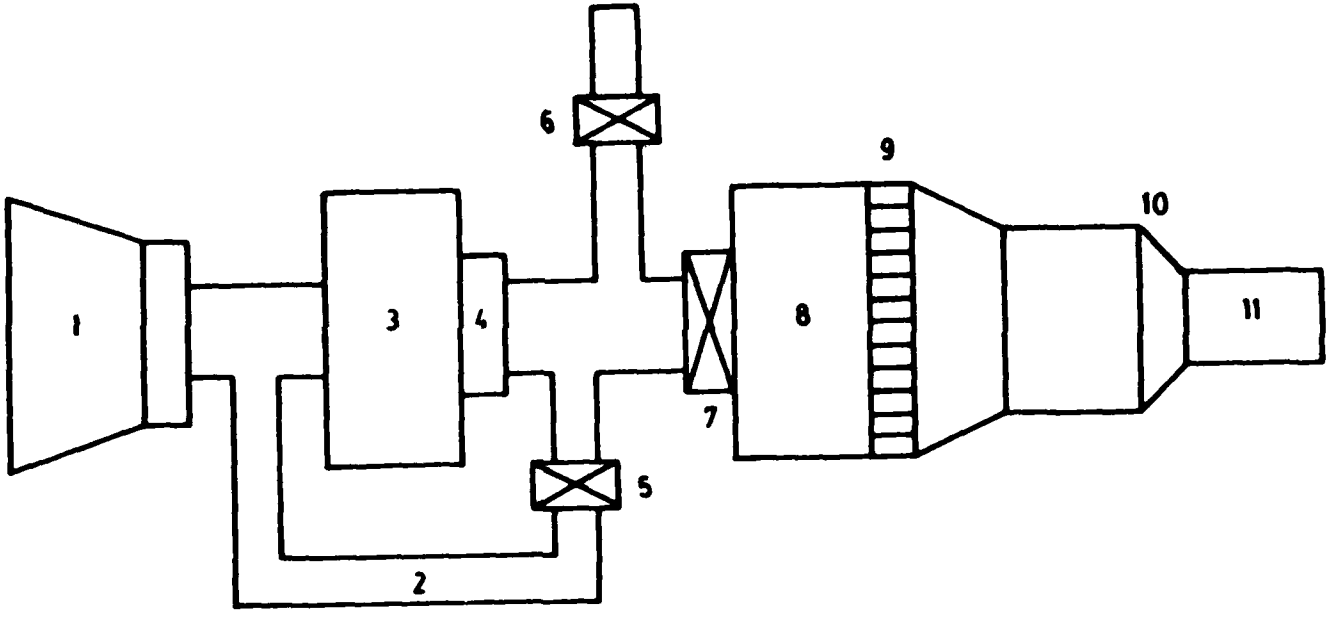

1. Compressor
2. Heat Exchanger Bypass
3. Heat Exchanger
4. Water Separator
5. Gate Valve
6. Gate Valve
7. Gate Valve
8. Plenum
9. Honeycomb
10. Converging Nozzle
11. Test Section

Figure 6. Flow System Schematic [Ref. 10]

Figure 7. Schlieren System and Laboratory Apparatus as Seen From Test Section Exhaust

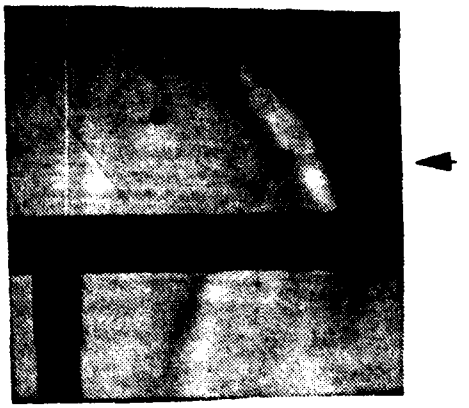

a.

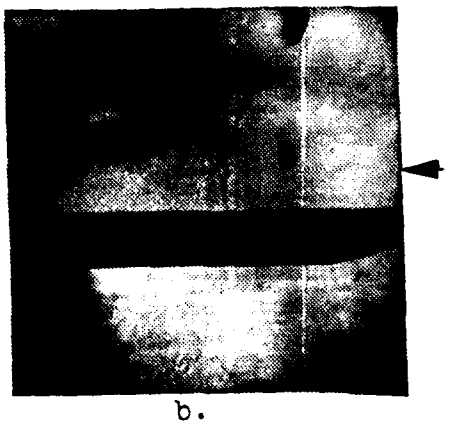

b.

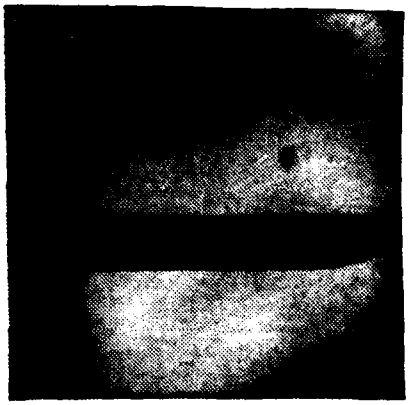

c.

a. No flow, candle held outside test section
b. No flow, heated soldering iron
c. Flow 33.1 ft/sec, heated soldering iron, flow from right to left

Figure 8. Cross-Flow Configuration, No Discharge

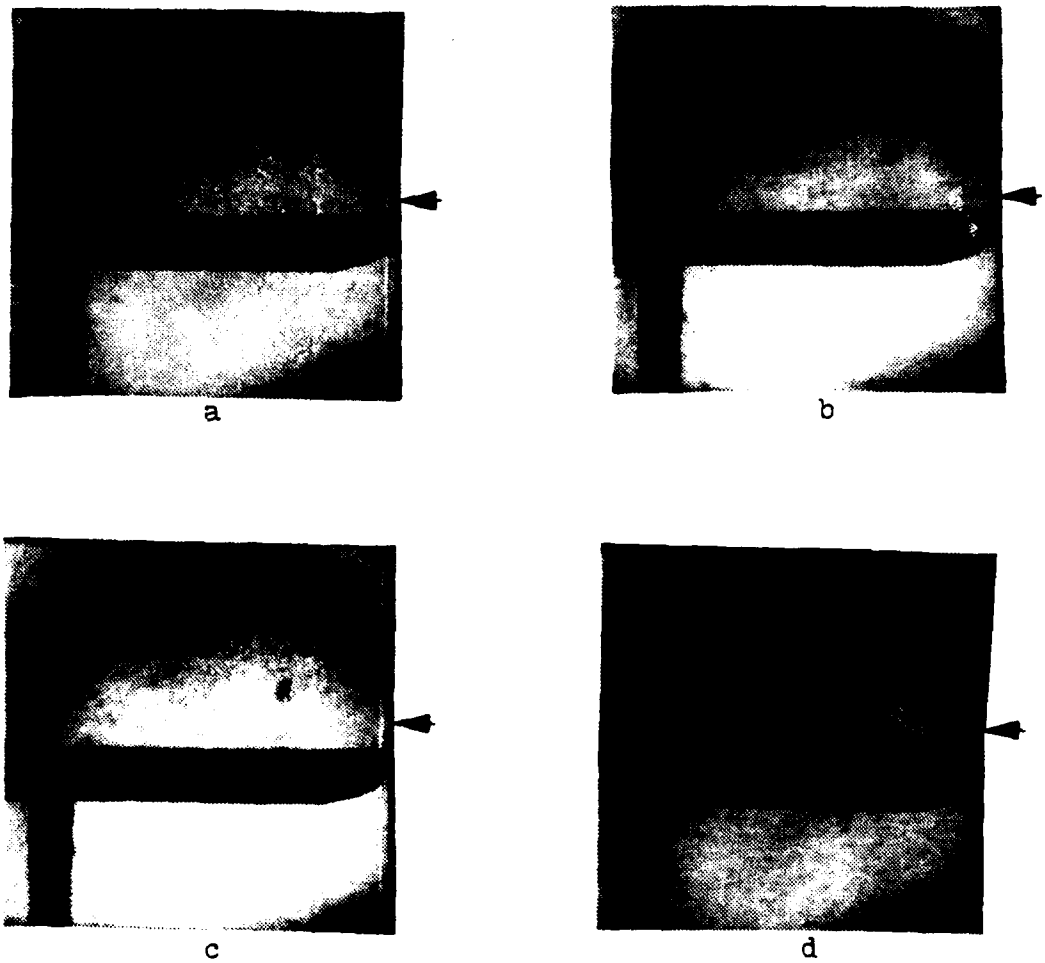

a. Flow 23.39 ft/sec, 19.5 kV, 1.2 mA
b. Flow 23.39 ft/sec, Just Prior to Breakdown
c. Flow 23.39 ft/sec, Just Prior to Breakdown
d. Flow 16.34 ft/sec, 19 kV, 1 mA

Figure 9. Cross-Flow Configuration, Flow From Right to Left

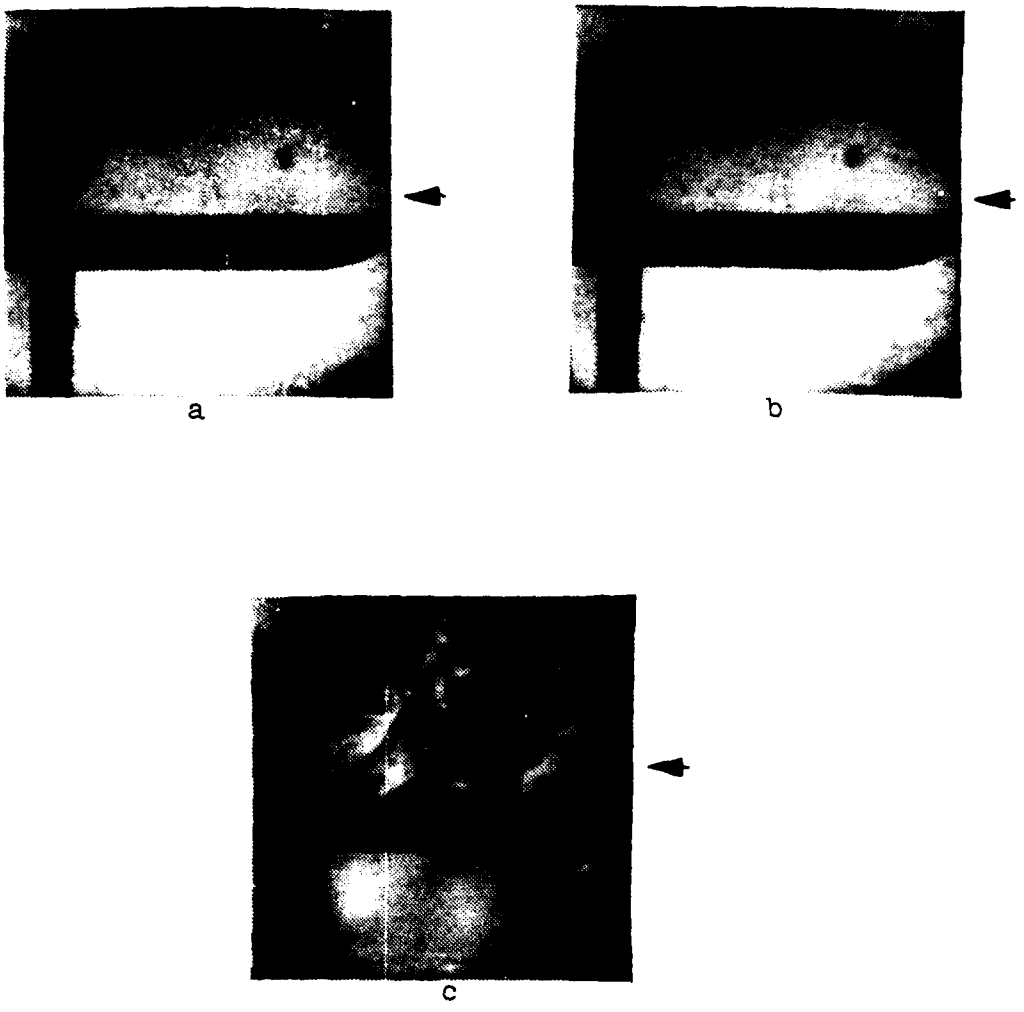

a. Flow 16.34 ft/sec, Immediately Prior to Breakdown
b. Flow 16.34 ft/sec, Immediately Prior to Breakdown
c. No Flow, Immediately After Breakdown

Figure 10. Cross-Flow Configuration

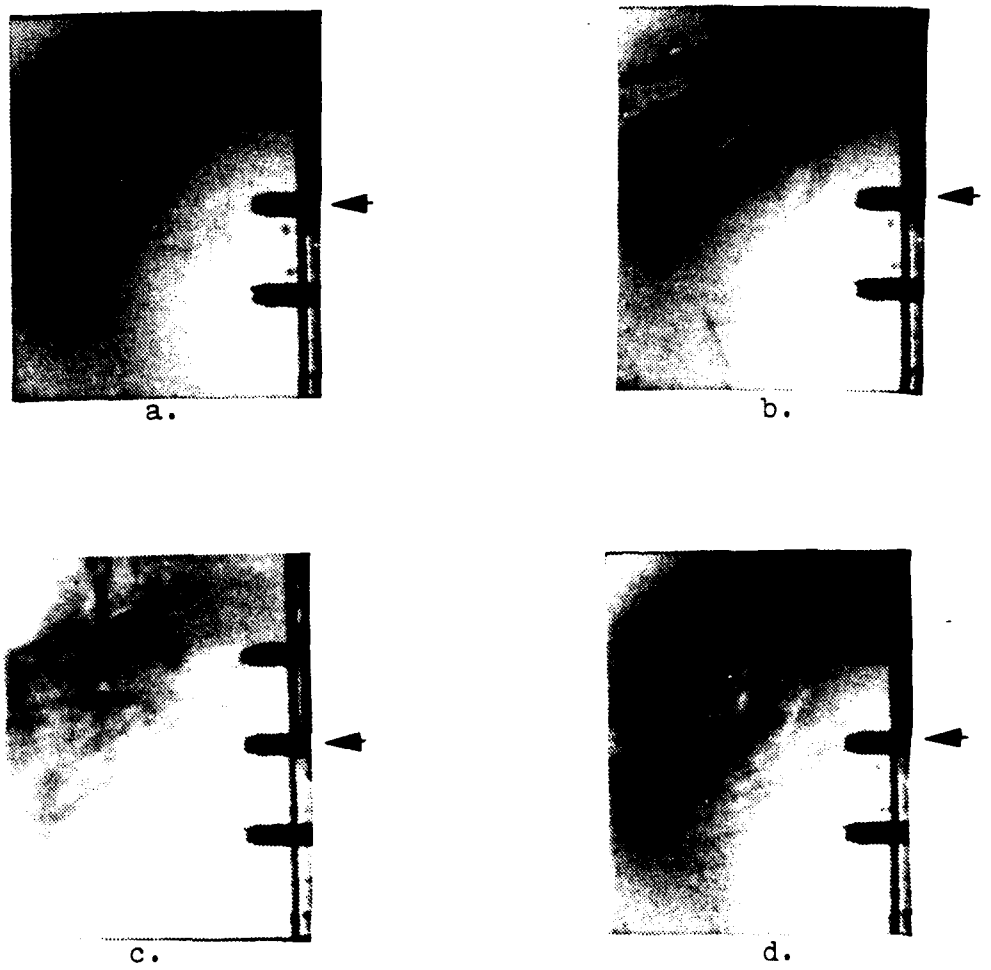

a. No Flow, 25 kV, 0.25 mA
b. No Flow, 26.5 kV, 0.8 mA
c. No Flow, 27.0 kV, 0.8 mA
d. No Flow, Immediately Prior to Breakdown

Figure 11. Parallel-Flow Configuration, No Flow, Various Discharge Conditions

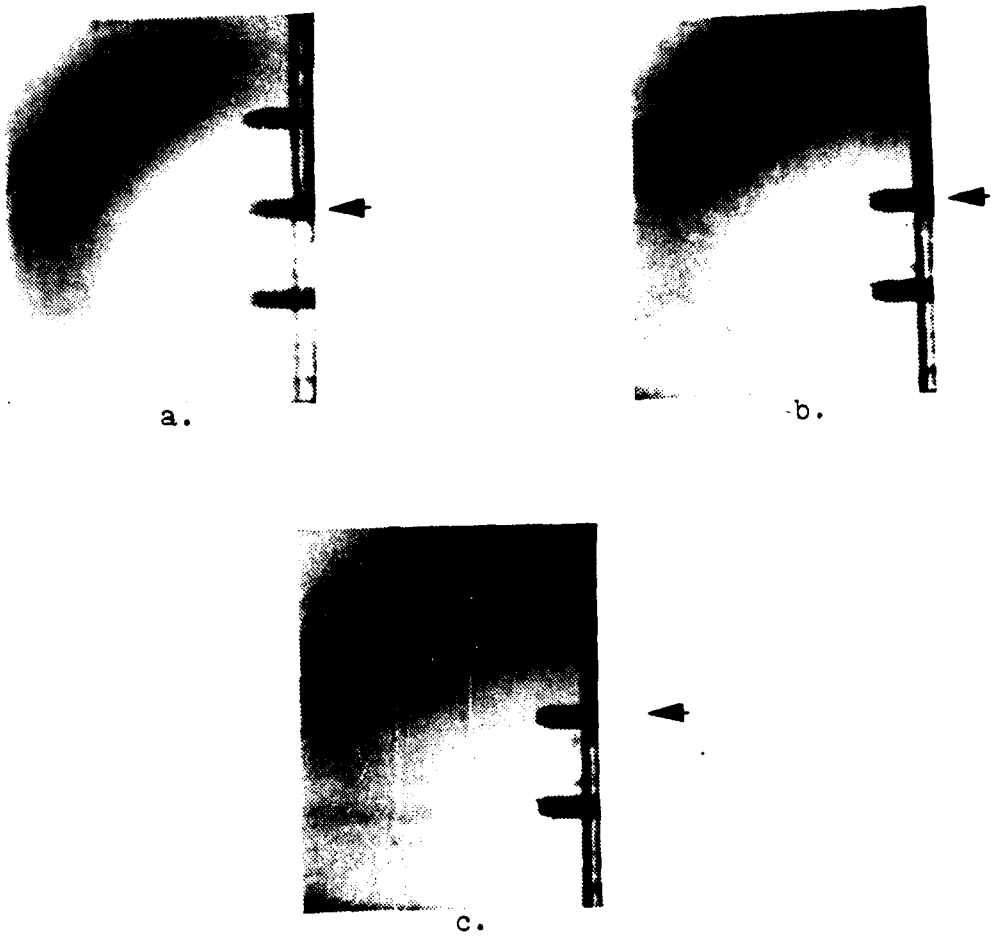

a. Flow 16.54 ft/sec, 26.5 kV, 0.8 mA
b. Flow 23.39 ft/sec, 28 kV, 0.8 mA
c. Flow 33.08 ft/sec, 28 kV, 0.8 mA

Figure 12. Parallel Flow Configuration, Various Conditions, Flow from Right to Left

LIST OF REFERENCES

1. Brown, C. O. and Davis, J. W., "Closed-Cycle Performance of a High-Power Electric-Discharge Laser", Applied Physics Letters, Vol. 21, pp. 480-481, 15 November 1972.

2. Post, H. A., Sub-Ambient Controlled Turbulence Effects on Discharge Stabilization for Laser Applications, M.S. Thesis, Naval Postgraduate School, September 1976.

3. Ibid., p. 9.

4. Ibid., p. 9.

5. Ibid., p. 10.

6. Eckbreth, A. C. and Owen, F. S., "Flow Conditioning in Electric Discharge Convection Lasers", The Review of Scientific Instruments, Vol. 43, pp. 995-998, July 1942.

7. Shwartz, J. and Wasserstrom, E., "The Role of Gas Flow and Turbulence in Electric Discharge Lasers", Israel Journal of Technology, Vol. 13, pp. 122-133, May 1975.

8. Shwartz, J. and Margalith, E., "On the Gas Temperature in Coaxial Electric-Discharge CO Flow Lasers", Journal of Applied Physics, Vol. 45, pp. 4469-4476, October 1974.

9. Shwartz, J. and Wasserstrom, E., p. 127.

10. Post, H. A., p. 4.

11. Ibid., p. 49.

12. Barto, J. L., Gasdynamic Effects on an Electric Discharge in Air, M.S. Thesis, Naval Postgraduate School, September 1976.

13. Ibid., pp. 14-18.

14. Ibid., pp. 84-90.

15. Ibid., p. 24.

16. Ibid., p. 31.

17. Ibid., p. 31.

18. Ibid., pp. 93-94.

19. Naval Postgraduate School Report NPS067-80-005, Study of Gas Dynamic Effects in Non-Uniform High Pressure Electrical Discharges, by J. L. Barto, August 1980.

20. Aunchman, L. J., Controlled Turbulence as a Design Criterion for Electric Discharge Convection Lasers, M.S. Thesis, Naval Postgraduate School, March 1974.

21. Biblarz, O., Barto, J. L. and Post, H. A., "Gas Dynamic Effects on Diffuse Electrical Discharges in Air", Israel Journal of Technology, Vol. 15, pp. 59-69, 1977.

22. Davis, C. H., Aerodynamic Stabilization of an Electric Discharge for Gas Lasers, M.S. Thesis, Naval Postgraduate School, September 1980.

23. Ibid., p. 93.

24. Wainionpaa, J. W., Electric Discharge Interaction in Parallel and Cross-Flow Electric Fields, M.S. Thesis, Naval Postgraduate School, September 1981.

25. Ibid., pp. 18-26.

26. Ibid., pp. 27-28.

27. Tucker, J. W., Effects of Acoustic Interference of a Flowing Gas on its Electrical Power Handling Capabilities, M.S. Thesis, Naval Postgraduate School, October 1982.

28. Wainionpaa, J. W., pp. 18-26.

29. Tucker, J. W., p. 28.

30. Babits, V. A., "Schlieren Photography", Photographic Applications in Science, Technology and Medicine, pp. 35-40, July 1972.

31. Merzkirch, W., Flow Visualization, Academic Press, 1974.

32. Wainionpaa, J. W., pp. 27-28.

33. Babits, V. A., pp. 35-40.

34. Reid, W. T., "Schlieren Photography", Kodak Pamphlet No. P-11, Eastman Kodak Co., 1960.

35. Vasil'ev, L.A., Schlieren Methods, trans. by A. Baruch, Israel Program for Scientific Translations, 1971.

36. Merzkirch, W., pp. 86-102.

37. Post, H. A., pp. 16-31.

38. Barto, J. L., pp. 19-32.

39. Wainionpaa, J. W., pp. 12-17.

40. Tucker, J. W., pp. 12-18.

41. Jenkins, F. A. and White, H. E., Fundamentals of Optics, pp. 74-77, McGraw-Hill1, 1957.

42. Kogelschatz, U. and Schneider, W. R., "Quantitative Schlieren Techniques Applied to High Current Arc Investigations", Applied Optics, Vol. 11, pp. 1822-1832, August 1972.

INITIAL DISTRIBUTION LIST

		No. Copies
1.	Defense Technical Information Center Cameron Station Alexandria, VA 22314	2
2.	Library Code 0142 Naval Postgraduate School Monterey, California 93940	2
3.	Office of Research Administration Code 012A Naval Postgraduate School Monterey, California 93940	2
4.	Chairman Department of Aeronautics Code 67 Naval Postgraduate School Monterey, California 93940	2
5.	Professor Oscar Biblarz Department of Aeronautics Code 67Bi Naval Postgraduate School Monterey, California 93940	4
6.	LCDR Terry Myers, USN HS-10 NAS North Island, California 92135	2